

Synthesis, sintering and characterization of PLZST perovskite prepared by a lactate precursor route

Lihong Xue^a, Qiang Li^{a,*}, Yiling Zhang^b, Rui Liu^a, Xihe Zhen^a

^a Department of Chemistry, Tsinghua University, Beijing 100084, China

^b Department of Material Science and Engineering, Tsinghua University, Beijing 100084, China

Received 24 August 2004; received in revised form 26 October 2004; accepted 12 November 2004

Available online 20 April 2005

Abstract

A lactate precursor route for synthesis of lanthanum-doped lead zirconate titanate stannate (PLZST) ceramic powders was developed, based on an aqueous solution of lactic acid and Pb^{2+} , La^{3+} , Zr^{4+} , Ti^{4+} , Sn^{4+} ions. The metal ions were brought in solution through complex formation with lactic acid. An amorphous precursor was prepared by dehydration of the soluble metal–ion–lactate complex solution. Heat treatment of the precursor at 650 °C for 2 h resulted in single phase perovskite PLZST powders. The effects of the ratio of lactic acid to mixed metal ions on the characteristics of PLZST powders were studied. The results showed that the powders prepared with the higher ratio (6:1) precursor consisted of finer particles with diameter of 45 nm and sintered readily to dense ceramics at the relatively low temperature of 1100 °C for 2 h. A typical antiferroelectric double polarization hysteresis loop was measured.

© 2004 Elsevier Ltd. All rights reserved.

Keywords: PLZST; Perovskites; Electrical properties; Precursor-organic

1. Introduction

Lead zirconate titanate stannate (PZST) ceramics and their modifications are recognized as prominent antiferroelectric materials due to their excellent electrical properties for practical applications.^{1–7} Since the discovery of the maximum 0.85% longitudinal strain in lanthanum-doped lead zirconate titanate stannate (PLZST) ceramics by Cross and co-workers,⁷ these ceramics have been investigated by various groups, for the purpose of improving their properties.^{8–15} It is well known that the properties of materials are strongly related to their preparation method and the starting materials. The conventional way to prepare PLZST ceramics is by solid-state method. This method often leads to compositional fluctuation and structural inhomogeneities. To overcome these problems, different methods have been developed to generate high purity, homogeneous, reactive PLZST ceramic powders,

such as coprecipitation,^{13,20} hydrolysis of metal alkoxides¹⁴ and other related methods.^{16–19}

Recently, a chemical method based on water-soluble chelated complexes as precursors to obtain the homogeneity of the metal ion distribution on the atomic level becomes very popular. In this synthesis route, citric acid is often used as a chelating agent for it can function as a ligand for many elements.^{21,22} And our experiment indicated that when using the citric acid process to obtain ceramic powders, the condensing temperature should be controlled under 70 °C until the formation of a highly viscous gel, otherwise, an irreversible precipitation took place and the solution would become a paste.²³ Lactic acid similar to citric acid can function as a ligand for many elements.^{24,25} However, contrary to citric acid, lactic acid is less sensitive to temperature during the condensing or dehydration process through our experiments. And lactic acid contains less carboxy group than citric acid, which results in less crosslinked network during condensing or dehydration process. This property not only prevents precipitation but also keep fluid, which leads to a more monodis-

* Corresponding author. Tel.: +86 10 62781694; fax: +86 10 62771149.
E-mail address: qiangli@mail.tsinghua.edu.cn (Q. Li).

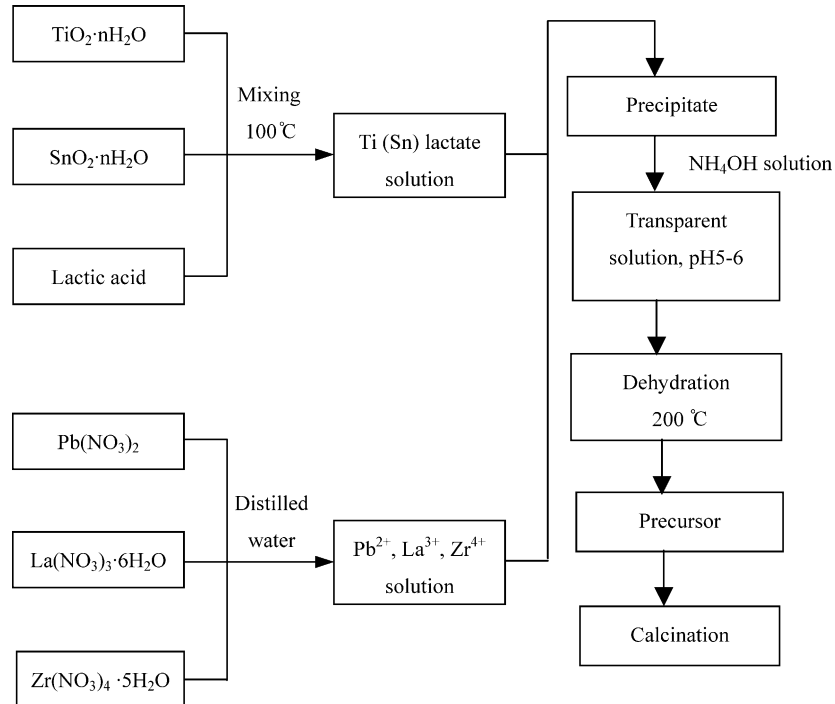


Fig. 1. Flow chart for preparation of PLZST ceramic powders.

persed precursor with a smaller aggregate particle size. So use of lactic acid as a chelating agent is more effective to produce fine PLZST ceramic powders. In this study, such a technique was used to prepare PLZST powders. Lactic acid was used as a chelating agent to keep the metal ions in homogeneous solution. The effects of the amount of lactic acid on the obtained powders were discussed, and the crystallinity behaviors during the precursor calcinations were investigated

as well. Additionally, the microstructures and electrical property of PLZST ceramics were studied.

2. Experimental

The composition of $\text{Pb}_{0.98}\text{La}_{0.02}(\text{Zr}_{0.66}\text{Sn}_{0.27}\text{Ti}_{0.07})\text{O}_3$ was chosen for the powders preparation. The raw ma-

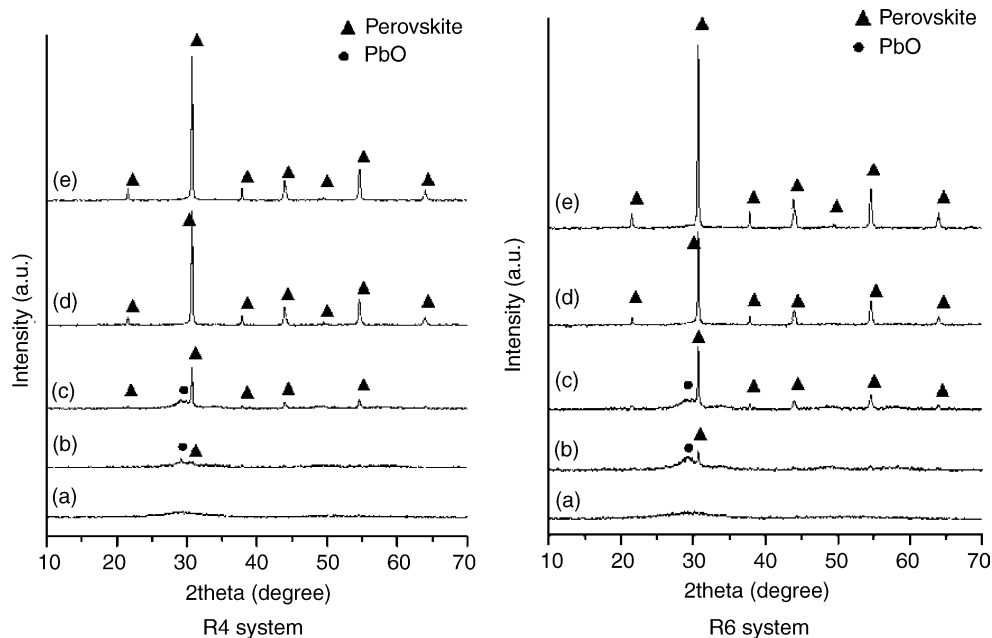


Fig. 2. XRD patterns of PLZST powders calcined at different temperatures: (a) precursor, (b) 450 °C, (c) 550 °C, (d) 650 °C, and (e) 750 °C for 2 h.

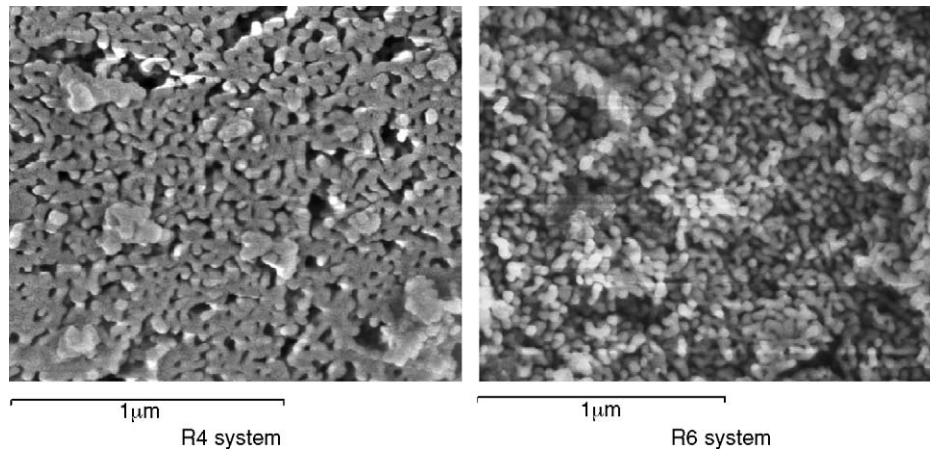


Fig. 3. SEM images of the powders calcined at 650 °C for 2 h.

materials were lead nitrate $\text{Pb}(\text{NO}_3)_2$, lanthanum nitrate $\text{La}(\text{NO}_3)_3 \cdot 6\text{H}_2\text{O}$, zirconium nitrate $\text{Zr}(\text{NO}_3)_4 \cdot 5\text{H}_2\text{O}$, hydrous titanium oxide $\text{TiO}_2 \cdot n\text{H}_2\text{O}$, hydrous stannium oxide $\text{SnO}_2 \cdot n\text{H}_2\text{O}$, and lactic acid. Hydrous titanium oxide was prepared in the laboratory from titanium tetrachloride (TiCl_4). Titanium tetrachloride reacted with ammonia solution to form precipitate hydrous titanium oxide. Similarly, hydrous stannium oxide was precipitated from tin tetrachloride ($\text{SnCl}_4 \cdot 5\text{H}_2\text{O}$). The respective hydrous oxides were then separated from their solutions by using filtration and washed with distilled water to make $\text{TiO}_2 \cdot n\text{H}_2\text{O}$ and $\text{SnO}_2 \cdot n\text{H}_2\text{O}$ free of chloride ions detected by acidified silver nitrate.

The procedure used to prepare PLZST powders by the lactate precursor method is shown in Fig. 1. Stoichiometric amounts of the prepared hydrous oxides of titanium and stannium were mixed with the required amount of lactic acid (for lactic acid variation studies, two systems were prepared in such a way in which the molar ratio of lactic acid to total metal ions in the starting solutions was maintained at 4:1 and 6:1, respectively; defined as the R4 system and the R6 system), and the resulting solution was heated ($\sim 100^\circ\text{C}$) with constant stirring. The hydrous oxides dissolved in lactic acid through complex formation and resulted in a clear yellow solution. Lead nitrate, lanthanum nitrate and zirconium nitrate were dissolved in distilled water to form a clear solution ($\text{pH} < 1$) and added into the previously prepared titanium stannium complex solution. At the beginning, a white gelatinous

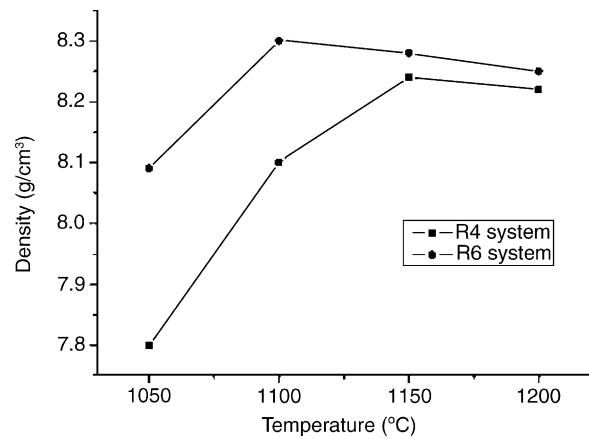


Fig. 4. Density of the PLZST ceramics as a function of sintering temperatures.

precipitate was formed. However, it dissolved when ammonia solution (NH_4OH) was added to give a final pH 5–6. The clear and homogeneous solution was heated at $\sim 200^\circ\text{C}$ for dehydration. During dehydration process, the complexing ability of lactic acid facilitated the homogeneous distribution of all metal ions in the solution and left sufficient flexibility for the system to exist homogeneously throughout the system without undergoing precipitation because polycondensation reaction happened in lactic acid and lactates. On complete dehydration of the solution, lactic acid and

Table 1

Average grain size and fracture characteristics of PLZST samples sintered at various temperatures

Lactic acid to metal ions ratio (<i>R</i>)	Sintering condition	Average grain size (μm)	Fracture characteristics
1:4	1050 °C/2 h	~1	Intergranular fracture
	1100 °C/2 h	~2	Intergranular fracture
	1150 °C/2 h	~2.5	Intergranular fracture with some transgranular fracture
	1200 °C/2 h	~9	Co-existence of transgranular and intergranular fracture
1:6	1050 °C/2 h	~1.5	Intergranular fracture with some transgranular fracture
	1100 °C/2 h	~2.5	Intergranular fracture with some transgranular fracture
	1150 °C/2 h	~6.5	Co-existence of transgranular and intergranular fracture
	1200 °C/2 h	Not measurable	Transgranular fracture

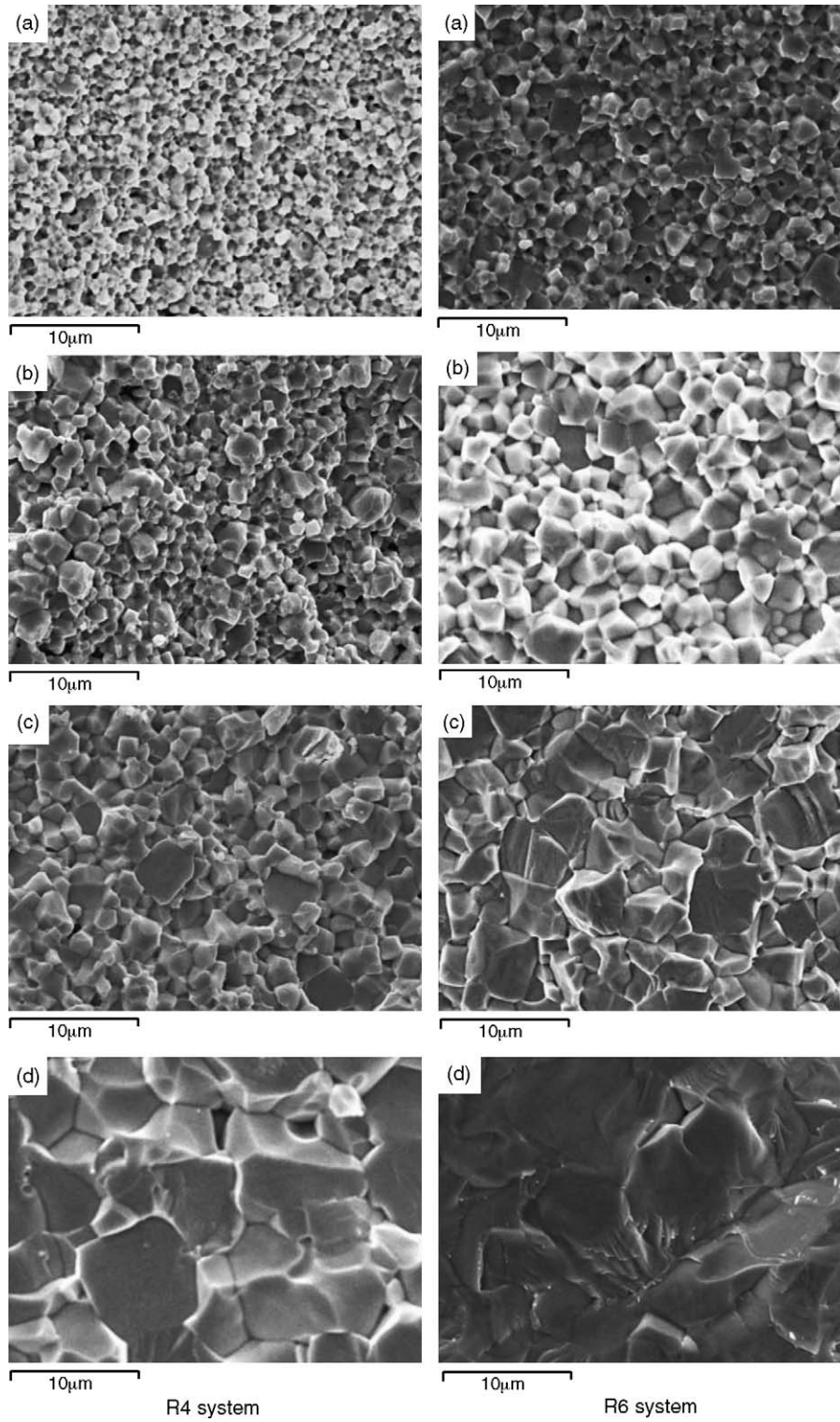


Fig. 5. SEM images of the PLZST ceramics sintered at various temperatures for 2 h: (a) 1050 °C, (b) 1100 °C, (c) 1150 °C, and (d) 1200 °C.

nitrate started to decompose leaving behind voluminous, black, fluffy, organic-based powders. These precursor powders were ground and calcined at various temperatures. The crystalline phase of the powders was identified by X-ray diffraction (XRD) analysis using Cu K α radiation. The particle size and morphology of powders were investigated by using scanning electron microscopy (SEM). To study the sinterability of the powders with pure perovskite phase, the calcined powders were subjected to axial pressing at 100 MPa to form pellets of 10 mm in diameter. The green pellets were sintered at 1050 °C, 1100 °C, 1150 °C and 1200 °C for 2 h, respectively, in a lead rich atmosphere. The lead atmosphere was provided by PbZrO₃ + 8 mol% ZrO₂ powders. SEM was used to investigate the microstructures of the sintered samples. The density was determined by the Archimedes method in water. The polarization–electric field (P – E) hysteresis loop was measured using a Sawyer–Tower circuit at room temperature.

3. Results and discussion

The lactate precursors prepared from the two systems (the R4 system and the R6 system) and powders calcined at different temperatures for 2 h were characterized by XRD as shown in Fig. 2. It indicates that the development of crystalline phase of powders is in the same trend for the two systems. The precursors are amorphous, and the PLZST perovskite phase is initiated at 450 °C, but PbO is detected. The heat treatment of the precursors at 650 °C for 2 h results in the formation of single-phase PLZST. The studies also reflect the growth of crystallinity in the powders with the increasing heat-treatment temperatures.

Fig. 3 shows SEM micrographs of the PLZST powders calcined at 650 °C for 2 h. It is shown that under the same formation temperature, the particle size decreases with an increase in the amount of lactic acid. The average particle diameter of the powders prepared from the R6 system is about ~45 nm while that of the R4 system is around 70 nm. And it

indicates that the lactate precursor route succeeds in controlling homogeneous grain size distribution.

The decrease of the particle size with increasing lactic acid amount is probably due to the dilution effect of the organic matrix during pyrolysis. Complete dehydration of the solution results in a loose and porous organic material. And during decomposition of the metal–ion–lactate complexes, metal oxide clusters with proper chemical homogeneity are formed, embedded in the porous material. Increasing the amount of lactic acid results in a larger amount of organic mass in the precursor and prevents aggregation of the metal oxide clusters during calcination. And the evolution of a large amount of gases (CO₂, H₂O, NH₃) during the pyrolysis helps not only to disintegrate the agglomerated particles but also to dissipate the heat of combustion, thus inhibiting the sintering of nanocrystalline powders.

To examine the sinterability of the nanosize powders produced in the two systems, the powders calcined at 650 °C for 2 h were pressed into the green pellets and sintered at 1050 °C, 1100 °C, 1150 °C, and 1200 °C for 2 h, respectively. The density of the PLZST ceramics as a function of sintering temperatures is plotted in Fig. 4. For the R6 system, the density increases from 1050 °C to 1100 °C, reaches a maximum value at 1100 °C and decreases a little after further sintering at higher temperature. The decrease in density of PLZST ceramics sintered at high temperature may be due to the grains growth and loss of PbO. For the R4 system, the maximum density value is obtained at 1150 °C.

Fig. 5 shows SEM micrographs of PLZST ceramics sintered at 1050 °C, 1100 °C, 1150 °C and 1200 °C for 2 h. The average grain size and fracture characteristics are summarized in Table 1. It indicates that the sintering temperature has influence on the morphology and microstructure of sintered PLZST ceramics. Samples sintered at lower temperatures contain smaller grains but also a considerable amount of pores in their structure, which explains the relatively low density measured for these samples. The grain size of the ceramics increases with an increase in sintering temperature. Compared with these two systems, the ceramics obtained from the R6 system have higher density

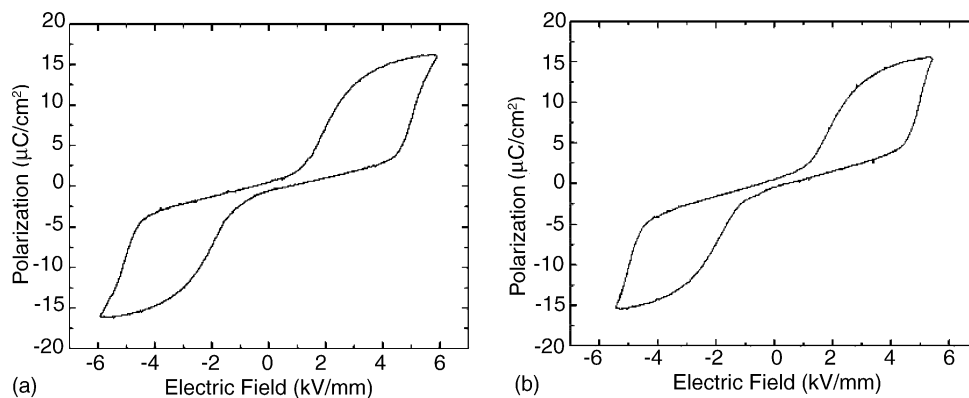


Fig. 6. P – E hysteresis loops of the PLZST ceramics: (a) R4 system, 1150 °C for 2 h and (b) R6 system, 1100 °C for 2 h.

than that obtained from the R4 system at the same temperature. It shows that the PLZST powders with the finer particle size can more readily be sintered than the coarser powders.

Fig. 6 shows the room temperature P – E hysteresis loops of the ceramics sintered at 1150 °C (the R4 system) and 1100 °C (the R6 system) respectively for 2 h. Typical antiferroelectric double hysteresis loops are observed. There is no distinct difference in the polarization properties of these two samples including the transformation field from AFE to FE and the reversing field FE–AFE. The coercive field, necessary to switch the polarization, is related with grain size; possible origin of this grain size effect is the presence of internal elastic stresses from grain boundaries and surrounding grains.²⁶ The stresses hinder the motion of domain walls, which controls the polarization switching.²⁷ So it is expected that the stress should be same in these two ceramics with similar grain size because the polarization properties of the two systems are similar.

4. Conclusions

PLZST powders were synthesized by a lactate precursor method. Well-crystallized PLZST powders were obtained at 650 °C for 2 h. The powders show nanometric-scale size and highly homogeneous grain size distribution. Comparing the two systems, the powders obtained from the R6 system have smaller primary particle size (~45 nm) than the powders prepared from the R4 system (~70 nm). The finer powders have better sinterability characteristics, and allow us to obtain dense ceramic bodies at lower temperatures than that of the coarser powders. For the R6 system, the density reaches a maximum value at 1100 °C while for the R4 system the maximum value was obtained at 1150 °C. For the two systems, typical antiferroelectric double hysteresis loops are observed with no distinct difference in the polarization properties.

Acknowledgement

The authors thank the National Natural Science Foundation of China, NNSFC 50272030, for the financial support of this work.

References

- Berlincourt, D., Jaffe, H., Krueger, H. H. A. and Jaffe, B., Release of electric energy in $\text{PbNb}(\text{Zr}, \text{Ti Sn})\text{O}_3$ by temperature and by pressure-enforced phase transitions. *Appl. Phys. Lett.*, 1963, **3**, 90–98.
- Uchino, K. and Nomura, S., Shape memory effect associated with the forced phase transition in antiferroelectrics. *Ferroelectrics*, 1983, **50**, 517–521.
- Nam, Y.-W. and Yoon, K. H., Phase formation and field-induced strain properties in Y-modified lead zirconate stannate titanate ceramics. *Jpn. J. Appl. Phys.*, 1999, **38**, 5544–5548.
- Yang, P. and Payne, D. A., Thermal stability of field-forced and field-assisted antiferroelectric-ferroelectric phase transformations in $\text{Pb}(\text{Zr}, \text{Sn}, \text{Ti})\text{O}_3$. *J. Appl. Phys.*, 1992, **71**, 1361–1367.
- Sternberg, A., Birks, E., Shebanovs, L., Klotins, E., Ozolinsh, M., Tyunina, M. et al., Phase transitions and properties of perovskite ferroelectric ceramics and films for certain applications. *Ferroelectrics*, 1999, **226**, 217–241.
- Pan, W. Y., Zhang, Q. M., Bhalla, A. and Cross, L. E., Field-forced antiferroelectric-to-ferroelectric switching in modified lead zirconate titanate stannate ceramics. *J. Am. Ceram. Soc.*, 1989, **72**, 571–578.
- Pan, W. Y., Dam, C. Q., Zhang, Q. M. and Cross, L. E., Large displacement transducers based on electric field forced phase transitions in the tetragonal $(\text{Pb}_{0.97}\text{La}_{0.02})(\text{Ti}, \text{Zr Sn})\text{O}_3$ family of ceramics. *J. Appl. Phys.*, 1989, **66**, 6014–6023.
- Blue, C. T., Hicks, J. C., Park, S.-E., Yoshikawa, S. and Cross, L. E., In situ X-ray diffraction study of the antiferroelectric–ferroelectric phase transition in PLSnZT . *Appl. Phys. Lett.*, 1996, **68**, 2942–2944.
- Park, S.-E., Pan, M.-J., Markowski, K., Yoshikawa, S. and Cross, L. E., Electric field induced phase transition of antiferroelectric lead lanthanum zirconate titanate stannate ceramics. *J. Appl. Phys.*, 1997, **82**, 1798–1803.
- Xu, B. M., Ye, X. H., Wang, Q. M., Pai, N. G. and Cross, L. E., Effect of compositional variations on electrical properties in phase switching $(\text{Pb}, \text{La})(\text{Zr}, \text{Ti}, \text{Sn})\text{O}_3$ thin and thick films. *J. Mater. Sci.*, 2000, **35**, 6027–6033.
- Essig, O., Wang, P., Hartweg, M., Janker, P., Nafe, H. and Aldinger, F., Uniaxial stress temperature dependence of field induced strains in antiferroelectric lead zirconate titanate stannate ceramics. *J. Eur. Ceram. Soc.*, 1999, **19**, 1223–1228.
- Xu, Z., Feng, Y. J., Zheng, S. G., Jin, A., Wang, F. L. and Yao, X., Phase transition and dielectric properties of La-doped $\text{Pb}(\text{Zr}, \text{Sn}, \text{Ti})\text{O}_3$ antiferroelectric ceramics under hydrostatic pressure and temperature. *J. Appl. Phys.*, 2002, **92**, 2663–2667.
- Lee, J. H. and Chiang, Y. M., Pyrochlore-perovskite phase transformation in highly homogeneous $(\text{Pb}, \text{La})(\text{Zr}, \text{Sn}, \text{Ti})\text{O}_3$ powders. *J. Mater. Chem.*, 1999, **9**, 3107–3111.
- Zhai, J. W. and Chen, H., Crystallization kinetics and dielectric properties in sol-gel derived $(\text{Pb}, \text{La})(\text{Zr}, \text{Sn}, \text{Ti})\text{O}_3$ ceramics. *J. Appl. Phys.*, 2003, **94**, 589–593.
- Viehland, D., Forst, D. and Li, J. F., Compositional heterogeneity and the origins of the multicell cubic state in Sn-doped lead zirconate titanate ceramics. *J. Appl. Phys.*, 1994, **75**, 4137–4143.
- Chen, M., Yao, X. and Zhang, L. Y., Preparation of $(\text{Pb}, \text{La})(\text{Zr}, \text{Sn}, \text{Ti})\text{O}_3$ antiferroelectric ceramics using colloidal processing and the field induced strain properties. *J. Eur. Ceram. Soc.*, 2001, **21**, 1159–1164.
- Kong, L. B., Ma, J., Zhang, T. S., Zhu, W. and Tan, O. K., Preparation of antiferroelectric lead zirconate titanate stannate ceramics by high-energy ball milling process. *J. Mater. Sci. Mater. Electron.*, 2002, **13**, 89–94.
- Zeng, Y. P., Zimmermann, A. and Zhou, L. J., Tape casting of PLZST tapes via aqueous slurries. *J. Eur. Ceram. Soc.*, 2004, **24**, 253–258.
- Zhou, L. J., Zimmermann, A., Aldinger, F. and Nygren, M., Preparation and properties of lead zirconate stannate titanate sintered by spark plasma sintering. *J. Am. Ceram. Soc.*, 2004, **87**, 606–611.
- Xue, L. H., Zhang, Y. L., Li, Q., Guo, Q. Y. and Liu, R., Preparation of PLZST with complex perovskite structure by coprecipitation. *J. Inorg. Mater.*, 2004, **19**, 566–570.
- Choy, J. H. and Han, Y. S., Citrate route to the preparation of nanometer size $(\text{Pb}, \text{La})(\text{Zr}, \text{Ti})\text{O}_3$ oxide. *Mater. Lett.*, 1997, **32**, 209–215.
- Pechini, M. P., Method of preparing lead and alkaline earth titanates and niobates coating method using the same to form a capacitor. US Patent, 3,330,697, 1967.
- Guo, Q. Y., Preparation of lead lanthanum zirconate stannate titanate (PLZST) relaxor anti-ferroelectric thin films. M.S. thesis, Tsinghua University, Beijing, China, 2004.

24. Hølted, C. H., Müller, A. and Rehbinader, D., *Lactic Acid*. Verlag Chemie International Research Association, Copenhagen-Der, 1971.
25. John, A. Dean, *Lange's Handbook of Chemistry (5th ed.)*. McGraw-Hill, New York, 1999, 8.96 pp.
26. Randall, C. A., Kim, N., Kucera, J. P., Cao, W. and Shrout, T. R., Intrinsic and extrinsic size effects in fine-grained morphotropic-phase-boundary lead zirconate titanate ceramics. *J. Am. Ceram. Soc.*, 1998, **81**, 677–688.
27. Arlt, G., The influence of microstructure on the properties of ferroelectric ceramics. *Ferroelectrics*, 1990, **104**, 217–227.